Novel Exploration of the Helium $(e,2e)$ Ionization Process

A. J. Murray and F. H. Read
Schuster Laboratory, Manchester University, Manchester, M13 9PL, United Kingdom
(Received 24 August 1992)

Absolute helium $(e,2e)$ differential cross sections have been measured over a more general range of directions of the outgoing electrons than has previously been attempted and at an incident energy for which all the complexities of exchange and capture processes, incoming and outgoing channel distortions, and short- and long-range correlations are present.

PACS numbers: 34.80.Dp

Atomic $(e,2e)$ angular correlation experiments provide the most exacting tests of ionization theories [1]. These tests are particularly severe for incident electron energies from a few eV to around 100 eV above threshold, because this range is too high for the Wannier model [2] to be valid and too low for the usual versions of the Born approximation [3] to be useful. Ionization in this energy range involves all the complexities of exchange and capture processes, incoming and outgoing channel distortions, and short- and long-range correlations. Previous $(e,2e)$ experiments have usually been at energies outside this range, and have usually been confined to coplanar geometry [4] or the recently introduced perpendicular plane geometry [5]. In this Letter we report on the first measurements in this energy region over an unrestricted range of scattering geometries.

The differential cross section $d^5\sigma/d\Omega_1 d\Omega_2 dE_1$ for the ionization process

$$e+A\rightarrow A^+ + e_1 + e_2 \tag{1}$$

is a function of four independent parameters, θ_1, θ_2, $\phi_1-\phi_2$, and E_1, assuming that the incident electron energy is fixed and that no polarization measurements are made (the energy E_2 of the other outgoing electron is not an independent parameter) [5]. In coplanar scattering experiments the parameter $\phi_1-\phi_2$ is set to zero, and of the remaining three, θ_2 is typically scanned for fixed values of θ_1 and E_1. In perpendicular plane experiments θ_1 and θ_2 are set to 90° and $\phi_1-\phi_2$ is scanned for a fixed value of E_1.

For the purposes of the present experiment we define an alternative set of parameters ξ_1, ξ_2, ψ, and E_1 as illustrated in Fig. 1. A general vector $\mathbf{r}$ can be written in terms of these parameters as follows:

$$\begin{aligned}\mathbf{r} &= \sin\theta\cos\phi\,\mathbf{i}+\sin\theta\sin\phi\,\mathbf{j}+\cos\theta\,\mathbf{k}\\ &= \sin\xi\,\mathbf{i}+\cos\xi\sin\psi\,\mathbf{j}+\cos\xi\cos\psi\,\mathbf{k}.\end{aligned} \tag{2}$$

The relationship between the parameter sets is thus given by

$$\tan\phi_i = \cot\xi_i \sin\psi, \tag{3}$$

$$\cos\theta_i = \cos\xi_i \cos\psi. \tag{4}$$

In the present apparatus [5,6] all four of the parameters can be varied. For these experiments we have chosen to let $\xi_1=\xi_2$ and $E_1=E_2$, giving a "doubly symmetric" differential cross section Σ. We then scan ξ_i for fixed values of ψ. Coplanar and perpendicular plane geometries correspond to $\psi=0°$ and 90°, respectively.

The measured differential cross section is independent of ψ when $\xi=90°$, giving a common normalization point as the angle ψ is varied. The measurements are placed on an absolute scale by normalizing against the coplanar results of Gélébart and Tweed [5,7].

The spectrometer is fully computer controlled and real-time computer optimized [6], with seventeen lens and deflector voltages involved in the optimization procedure. The system is actively maintained at its optimum for continuous periods of up to four weeks, resulting in data that are more reliable and consistent than were previously obtainable with manual control and optimization [6]. The electron gun has a resolution of 600 meV and

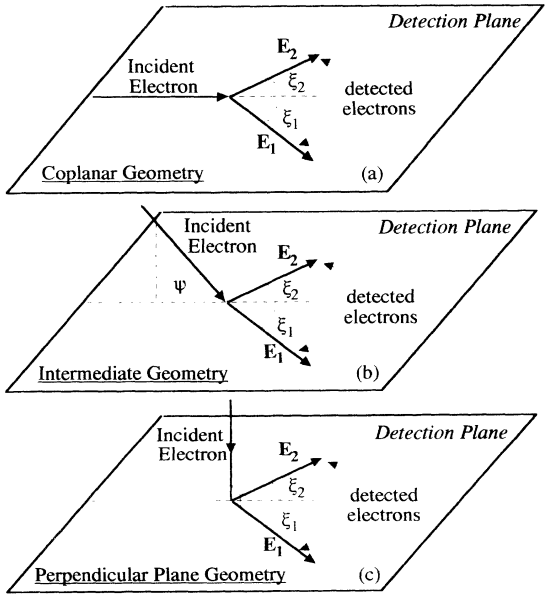

FIG. 1. Evolution from coplanar to perpendicular plane geometry [(a)–(c)]. ψ is the angle between the detection plane and the incident electron beam direction. ξ_1 and ξ_2 are the electron scattering angles in the detection plane.

focuses a current of 4 μA to a beam of 1 mm diameter at the interaction region, with zero beam angle and a pencil angle of approximately 2°. Two hemispherical deflection analyzers rotate in a horizontal detection plane, each analyzer being preceded by a triple-cylinder input electrostatic lens that has an acceptance half-angle of 3°.

Nine gun angles have been used for an incident energy of 44.6 eV (20 eV above the helium ionization threshold). For $\psi < 70°$ the analyzers were constrained by the presence of the electron gun to $35° < \xi < 125°$, whereas for ψ between 70° and 85° the analyzers were constrained to $35° < \xi < 140°$. The perpendicular plane geometry ($\psi = 90°$) afforded the greatest angular freedom with $25° < \xi < 155°$. Figure 2 shows the experimental results with numerical fits added to aid in the description (see below). The results are normalized at the point $\xi = 90°$, where the differential cross section (DCS) was determined to be $\Sigma = (9.6 \pm 4.2) \times 10^{-3}$ a.u.

A number of interesting features are apparent. First, it can be noted that the coplanar ($\psi = 0°$) forward scattering peak is smaller than the backward scattering peak, as previously found at an incident energy of 50 eV and below [4], indicating that simple "binary" collision processes are not dominant at this energy. As ψ increases from 0° to 90°, the forward scattering peak retains its identity and position, whereas the backward scattering peak evolves into the peak at $\xi = 90°$ in the perpendicular plane. A high-angle tail develops in the backscatter peak and evolves into the peak at $\xi \approx 140°$ in the perpendicular plane. The minimum in coplanar geometry located at $\xi \approx 80°$ evolves into a minimum at $\xi \approx 55°$ in the perpendicular plane geometry. A symmetry relationship that can be used to generate results for $\psi = 90°$ to 180° is

$$\Sigma(180° - \xi, 180° - \psi) = \Sigma(\xi, \psi), \tag{5}$$

provided that $\xi_1 = \xi_2$ and $E_1 = E_2$, as in the present experiments. Using this we see that as ψ increases from 90° to 180°, the backscatter peak evolves into the forward scatter peak and vice versa. Finally it can be noted that the peak intensity variation from coplanar to the perpendicular plane geometry is only 20:1, allowing the results to be presented on a linear scale.

The range of geometries used in this study allows a three-dimensional map of the differential cross section to be produced, since results obtained at a particular value of ψ characterize a two-dimensional "slice" of the complete doubly symmetric differential cross section. The 3D map possesses two planes of reflection symmetry due to the indistinguishability of the detected electrons and the unpolarized nature of the electron beam and atomic source. These symmetry planes are the detection plane and the plane of the rotating incident electron beam.

The 3D map has been generated by fitting the data shown in Fig. 2 by the expression

$$\Sigma(\xi, \psi) = \Sigma(\xi = 90°) + \sum_{i=0}^{8} \sum_{j=1}^{9} c_{ji} \cos^i(\psi) \cos^j(\xi) . \tag{6}$$

This has the required reflection symmetries and also satisfies relationship (5). Furthermore, it has been constrained to give a differential cross section that is negligible at $\xi = 0°$ and 180° for all angles ψ as required since postcollisional interactions between equally energetic electrons traveling initially in the same direction force the electrons to move away from each other, resulting in a very small probability of detecting the electrons together. The fitted differential cross section, a function of the detection plane angle ξ and gun angle ψ, was finally remapped into the conventional (x,y,z) coordinate system in which the incident beam direction defines the z

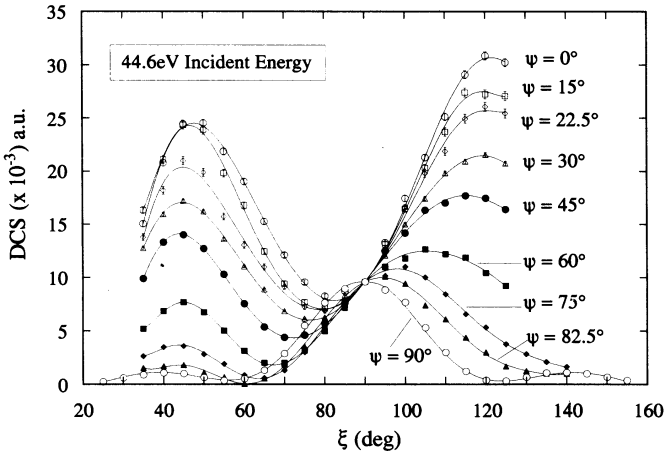

FIG. 2. The doubly symmetric helium $(e,2e)$ differential cross section (DCS) as a function of ξ and ψ at an incident energy of 44.6 eV, normalized to the common point at $\xi = 90°$.

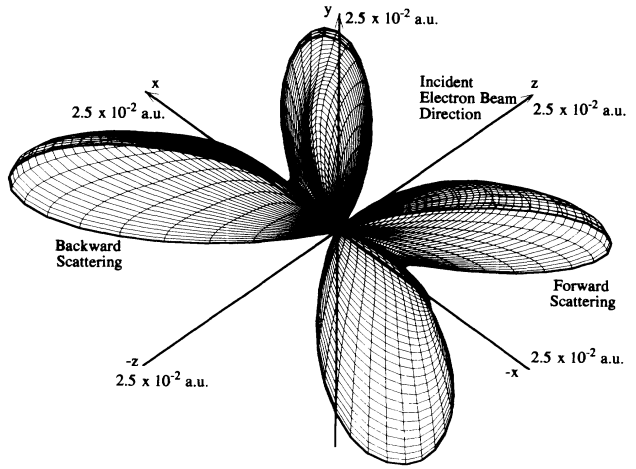

FIG. 3. The 3D map of the DCS calculated from the results in Fig. 2. The viewing direction is at 45° to the x-z plane rotated at 45° around the y axis. The incident electron beam direction is the $+z$ direction. The linear axes extend to 2.5×10^{-2} a.u. Coplanar geometry yield is highlighted, whereas the noncoplanar yield is shown for positive values of y only.

axis.

Figure 3 illustrates the result of this procedure. The differential cross section surface is only shown above the coplanar (x-z) scattering plane, since the surface possesses reflection symmetry in this plane. The viewing angle is at 45° to the x-z plane and is rotated 45° around the y axis. The surface is seen to have reflection symmetry in the y-z (gun angle) plane, necessary due to the indistinguishability of the electrons. The axis limits are set to 2.5×10^{-2} a.u. and the coplanar differential cross section is highlighted. The evolution of the forward scattering coplanar lobe into the lower perpendicular plane lobe can be seen, since there is a global minimum in this half of the x-z plane, corresponding to the minimum between forward and backscatter peaks in Fig. 2.

Noncoplanar theoretical calculations [8,9] using second and distorted-wave Born models exist only for scattering into the perpendicular plane geometry. The coplanar results [4] that straddle the present coplanar results have been modeled using a distorted-wave Born approximation [8], but there is no agreement with experiment. No calculations exist with which to compare the intermediate plane results presented here.

Further experiments where the symmetry adopted in these experiments is relaxed are at present being pursued. These include measurements where $E_1\neq E_2$, measurements where $\xi_1\neq\xi_2$, and measurements where $E_1\neq E_2$ and $\xi_1\neq\xi_2$.

The Science and Engineering Research Council is acknowledged for financial support of this work and for providing a research associateship (A.J.M.) during this period.

[1] A. Lahmam-Bennani, J. Phys. B **24**, 2401 (1991).
[2] F. H. Read, in *Electron Impact Ionisation*, edited by G. Dunn and T. Märk (Springer, Berlin, 1985), pp. 42–88.
[3] F. W. Byron and C. J. Joachain, Phys. Rep. **179**, 211 (1989).
[4] T. Rösel *et al.*, J. Phys. B **24**, 3059 (1991).
[5] A. J. Murray *et al.*, J. Phys. B **25**, 3021 (1992).
[6] A. J. Murray *et al.*, Rev. Sci. Instrum. **63**, 3349 (1992).
[7] F. Gélébart and R. J. Tweed, J. Phys. B **23**, L641 (1990).
[8] X. Zhang *et al.*, Z. Phys. D **23**, 301 (1992).
[9] F. Mota-Furtado and P. F. O'Mahony, J. Phys. B **22**, 3925 (1989).